Deployment Experiment for Ultralarge Solar Sail System (UltraSail)

Byoungsam Woo,* Kevin M. Ertmer,† and Victoria L. Coverstone‡
University of Illinois at Urbana–Champaign, Urbana, Illinois 61801
and
Rodney L. Burton,§ Gabriel F. Benavides,¶ and David L. Carroll**
CU Aerospace, Champaign, Illinois 61820

UltraSail is a next-generation high-payoff system with very large (kilometers-squared class) solar sails enabling high payload mass fractions for high Delta-V. One of the primary innovations is the near elimination of sail supporting structures by attaching each blade tip to a formation-flying tip satellite. To design the deployment of kilometers-long blades by centrifugal force provided by tip satellites, the peel force of the blade material must be known. In this research, an experiment to determine the force necessary to deploy a stowed film in a vacuum was designed, fabricated, and operated for various CP-1 polyimide film samples, including uncoated, aluminum-coated, and uncoated but conductive film. Results for uncoated film samples were heavily dependent on vacuum levels, with very high forces observed at low pressures due to electrostatic charge buildup. However, for the coated film and conductive film samples, the types most likely to be used on an UltraSail mission, preliminary results show that the peel forces are negligibly small. This small peel force is critical for the successful, simple, and efficient deployment of the UltraSail system. A potential problem associated with trapped air between film layers was identified by the experiment, and a future winding scheme will guard against this issue.

Nomenclature

b	=	sail film width, m
c	=	chord (width) of solar sail blade, m
Delta-V	=	change in velocity by any thrusting mechanism
FR	=	force ratio (F_{cent}/F_z)
F_{cent}	=	centrifugal force acting on blades and tip satellites, N
$F_{cent-deploy}$	=	centrifugal force acting on blades and tip satellites during deployment of blades, N
$f_{friction}$	=	friction force from the bearing at lever arm pivot
$f_{gravity_{film mass}}$	=	gravitational force from mass of film sample between reels
$f_{gravity_{lever arm}}$	=	lever arm restoring force from pendulum motion
F_{peel}	=	force required to peel unit width of sail film from reel, N
f_{roller}	=	force in opposite direction of f_{sensor} on roller by tension of film, N
f_{sensor}	=	force measured by force sensor in experiment, N
F_{unroll}	=	force to unroll sail film from reel, N
f_{wrap}	=	true force acting on roller by tension of film, N
F_z	=	solar pressure force along UltraSail rotation axis, N
L	=	length of solar sail blade measured from reel, m
L_{boom}	=	length of boom that connects hub and reel, m
M	=	mass of hub satellite, kg
m_{blade}	=	film mass for one blade, kg
m_{bs}	=	mass of tip satellite and unrolled portion of blade, kg
P_0	=	pressure on a perfectly reflecting surface at 1 AU, N
R	=	lever arm ratio
T	=	tension on the film, N
V_{tip}	=	tangential velocity of tip satellites, m/s
γ	=	angle between sun–spacecraft line and UltraSail rotation axis (sun angle), rad
ζ	=	angle from line connecting hub and tip satellite and x axis (deflection angle), rad
θ_p	=	peeling angle of film from reel, rad
θ_0	=	angle between peeling point and horizontal line, rad
θ_1	=	wrap angle in sensing roller between arriving point and f_{roller}, rad
θ_2	=	wrap angle in sensing roller between departing point and f_{roller}, rad

I. Introduction

ONE of the acknowledged problems with solar sails has been the large sail area needed for adequate acceleration. Solar sails accelerate a spacecraft by harnessing solar radiation and exchanging photon momentum for spacecraft momentum. Because the solar pressure force is extremely small, solar sails necessarily entail large areas. The sails replace the typical chemical or electric propulsion devices and must have mass similar to or lower than a viable low-thrust propulsion alternative. An ideal solar sail material is exceptionally thin, and it perfectly reflects the entire spectrum of solar radiation. Recent advances in thin films have produced several different materials considered suitable for solar sail applications [1,2]. These films are typically plastic, with a very thin reflective coating, with total thicknesses on the order of 2–25 μm, and with
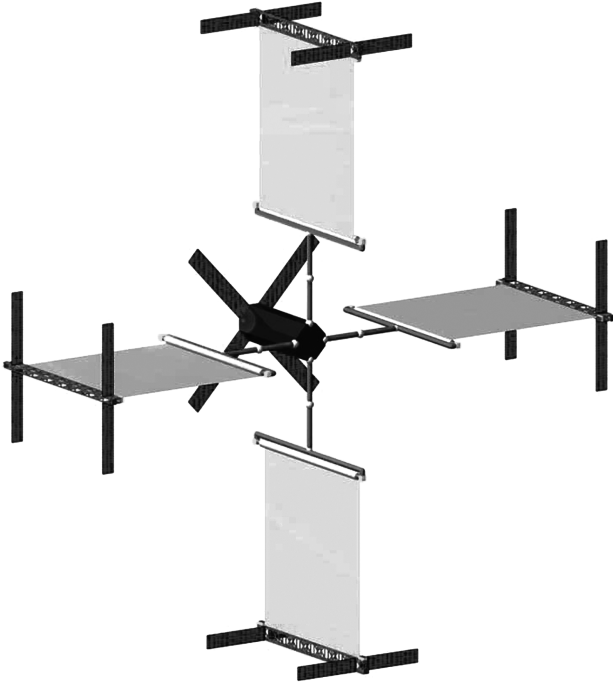
Fig. 1 Rendering of UltraSail concept.

Fig. 2 Definition of parameters and coordinate (z is the rotation axis).

areal densities of 2–35 g/m^2. Current solar sail materials include Mylar, Kapton, and various polyimide films. With the current maturity in solar sail material technologies, the problem of deployment and maintaining rigidity of the system needs to be addressed. Conventional solar-sailing spacecraft designs use large booms to deploy and support the thin film of reflective material. These boom-deployed schemes are limited in size by the penalties associated with the boom mass compared with the sail area, specifically Euler column buckling of the booms. It logically follows that eliminating the booms could provide larger sail area, higher thrust, and lower areal density, resulting in higher acceleration and higher payload mass fractions. Removing these support structures is at the core of the UltraSail concept [3].

As shown in Fig. 1, there is a hub satellite containing the payload in the UltraSail system. Attached to the hub would be several blades of few-micrometer-thick reflectively coated polyimide film that unroll from a storage reel with the help of a tip satellite that is attached to the end of each blade. The UltraSail system will be stowed in a launch vehicle with all blades wound up on storage reels. After separation from the launch vehicle, the UltraSail starts deploying its blades as shown in Fig. 1. During the deployment of the blades, the formation-flying tip satellites spin up the blade system to create a spin-stabilized controllable solar sail system, with sail areas on the order of 0.1 km^2. In the UltraSail mission, one of the most difficult challenges is the deployment of the 0.5-km-long blade. The current design specification of the UltraSail mission is given in Table 1 [3,4]. The deployment is designed to provide the desired final angular velocity

to the blade system (blade and tip satellite), as well as the unrolling of blades from the storage reels. The few-micrometer-thick sail film stored on the reel is unrolled by centrifugal force in a controlled manner until fully deployed. The final angular velocity of the blade system is designed to maintain the sun angle on the blade to a preset value by balancing the solar pressure and the centrifugal force. During the deployment, the angular velocity of the blade system is provided by the initial spin of the spacecraft, tangential acceleration by the tip satellite thrusters, and windmill-like cyclic pitching of the blade [5]. The five-axis cold or warm gas thrusters on tip satellites are also used for attitude control and maneuver, as well as for the deployment.

II. Deployment Dynamics

The balance between the solar pressure and the centrifugal force is described by a ratio of the two forces. The force ratio is defined to be a ratio of the centrifugal force on the blade system to the solar pressure force in the direction of the Ultrasail rotation axis (axis z in Fig. 2). Increasing the force ratio decreases the deflection angle (ζ) of the blades, which is desirable to maximize the sail area facing toward the sun. However, increasing the force ratio increases the angular velocity of the UltraSail, thereby increasing the propellant needed to accelerate the tip satellites. The force ratio determines the equilibrium deflection angle of the blade system. From a previous work, the optimal force ratio was determined to be three to five, depending on the mission length, meaning the centrifugal force is three to five times larger than the solar pressure [3].

In this paper, it is assumed that the optimal force ratio is maintained during the deployment of the blade system. Designing the profile of the force ratio variation during the deployment is out of the scope of this research. However, the advantages of maintaining the optimal force ratio during the deployment include the following:

1) The deflection angle remains constant throughout the deployment.

2) There is no need to command a large velocity change of the tip satellite at the end of the deployment. To maintain the force ratio, the velocity of the tip satellite should be controlled. The definition of the force ratio is given in Eq. (1):

$$FR = \frac{F_{\text{cent}}}{F_z} \qquad (1)$$

The solar pressure force F_z is computed by Eq. (2) with deflection angle ζ:

$$F_z = P_0 c L(t) \cos^2(\gamma - \zeta) \cdot \cos \zeta \qquad (2)$$

As shown in Fig. 1, the reel is deployed from the hub with a boom and the unrolling begins from the reel. Therefore, the initial deployment position is L_{boom} from the hub satellite. With the boom length considered, the centrifugal force is described as in Eq. (3):

Table 1 Deployment system specification

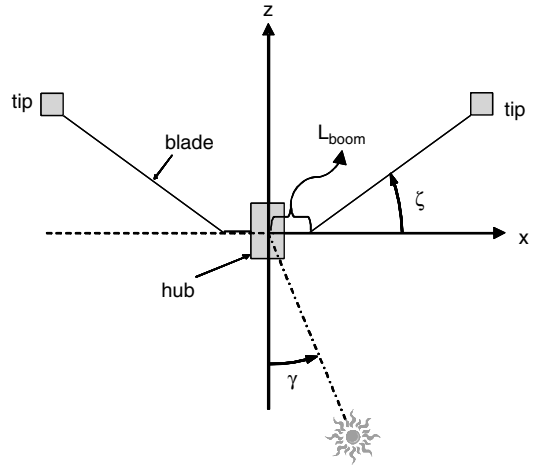| Specification	Value
Blade length (L)	500 m
Blade width (b)	5 m
Sail thickness	5 μm
Hub satellite mass	50 kg
Tip satellite mass	31.1 kg
Initial deployment position	5 m from center
(L_{boom}: boom length)	of hub satellite
Initial angular velocity of spacecraft	1 deg / min
Mission time	8 years
Maximum deployment time	<10 h

$$F_{\text{cent}} = m_{bs}(t) \frac{V_{\text{tip}}^2}{L(t)\cos\zeta + L_{\text{boom}}} \qquad (3)$$

where L_{boom} is 5 m, and $m_{bs}(t)$ is the mass of the blade system that increases as more blade is unrolled, since the mass shifts from the reel to the deploying blade system [4]. From Eqs. (1–3), the V_{tip} to maintain the optimal force ratio is derived as in Eq. (4):

$$V_{\text{tip}} = \left[\frac{L(t)\cos\zeta + L_{\text{boom}}}{m_{bs}(t)} \cdot FR \cdot F_z \right]^{1/2} \qquad (4)$$

It is assumed that the moment of the reel is not a factor in computing V_{tip}, because the rotation of the reel is synchronized by a motor rather than being turned by the blade itself. However, the force to unroll the blade film from the reel needs to be added to the required centrifugal force during the deployment. During the deployment, Eq. (1) is modified as in Eq. (5):

$$F_{\text{cent-deploy}} = FR \cdot F_z + \frac{F_{\text{unroll}}}{\cos\zeta} \qquad (5)$$

and the required V_{tip} is increased, as given in Eq. (6):

$$V_{\text{tip}} = \left[\frac{L(t)\cos\zeta + L_{\text{boom}}}{m_{bs}(t)} \left(FR \cdot F_z + \frac{F_{\text{unroll}}}{\cos\zeta} \right) \right]^{1/2} \qquad (6)$$

The F_{unroll} is used to peel the film from the roll, and it is related to the peel force F_{peel} with peeling angle θ_p and film width b, as shown in Eq. (7):

$$F_{\text{unroll}} = \frac{F_{\text{peel}} \cdot b}{1 - \cos\theta_p} \qquad (7)$$

The peel force is the force required to peel one layer of film from itself. To minimize F_{unroll}, the peel force should be minimized and the peeling angle should be close to 90 deg. The peeling angle can be controlled close to 90 deg by an unrolling mechanism, but the peel force can vary enormously depending on the characteristics of the film material. Therefore, a ground experiment is designed to measure the peel force of various sail film samples in vacuum.

III. Vacuum Deployment Experiment

The purpose of the vacuum deployment experiment is to validate the concept of unrolling a stored thin film in a vacuum and to identify anything that might help or hinder this process. The key parameter of interest is the peel force. If the peel force is too high, then a simple deployment using centrifugal force would not be possible. Furthermore, even if higher thrust alternatives were used to deploy the sails, there is a level of peel force that becomes problematic from a structural standpoint. The film samples used in the experiment are variants based on LARC CP-1 polyimide films developed by NeXolve Corporation [1]. The breaking strength of CP-1 film in tension is 100 MPa. Incorporating this material strength into the baseline design, with a safety factor of 4, the tensile force on any given section of the film must be less than 250 N, assuming the load is uniformly distributed across the film width [4]. Also, the amount of propellant needed to reach 250 N by centrifugal force is prohibitively high.

Additionally, the family of thrusters selected for the UltraSail tip satellites (five-axis cold or warm thrusters) are on the order of millinewtons and micronewtons, meaning that the capability of the thrusters in providing the peel force as well as the desired centrifugal force is limited. Therefore, knowing the peel force is critical to the continued evolution and development of the UltraSail concept. The vacuum deployment experiment is devised to isolate the peel force in a vacuum by simulating the unrolling of the stored sail material in the space environment. At the same time, the experiment allows qualitative observation of the deployment process. Finally, the experiment is designed to be portable enough to be placed onboard a microgravity simulation aircraft, with minimal modification.

A. Adhesive Forces in Sail Film

Forces that cause surfaces to stick together are not well known. Many studies have been performed on surface forces as they relate to friction, which has given rise to the field of tribology. However, these frictional forces are not present in the unrolling of a thin film. Another possible attractive force that can give rise to a peel force is intermolecular force. Intermolecular forces are not well understood either and are very dependent on surface geometry and environmental factors. Intermolecular forces can become significant for surfaces and particles in close proximity (nanometer separation). In any true surface, however, very few particles ever come this close to each other. The contact of two surfaces is produced by two very rough surfaces that touch each other at only a few tall spots. Therefore, although the intermolecular forces may be strong, they are only strong over a very minute portion of the surface [6].

Finally, there are electrostatic forces. Electrostatic force levels are orders of magnitude greater than intermolecular forces at distances greater than the subnanometer level. Intermolecular forces rapidly drop to nearly zero upon separation. However, in order for electrostatic forces to be present, charge must develop on the surfaces. As will be described below, charge does in fact build up on the surface of the samples of nonconductive thin film. However, the way in which such charge builds up on a nonconductor is not known. It is heavily dependent on surface conditions on the macro and atomic scales, as well as test conditions such as the humidity and pressure. It can be so unpredictable that, even under the most stringent and controlled experiments to measure charge production, no repeatability is obtainable. In short, the nature of the forces that cause the peel force is beyond the scope of this research. The goal of this experiment is to determine if a peel force exists and, if so, to find its dependence on deployment speed for four different film samples.

B. Experiment Design

Figure 3 shows the geometry of the peel force measurement apparatus, and Fig. 4 shows the actual apparatus. In this setting, the
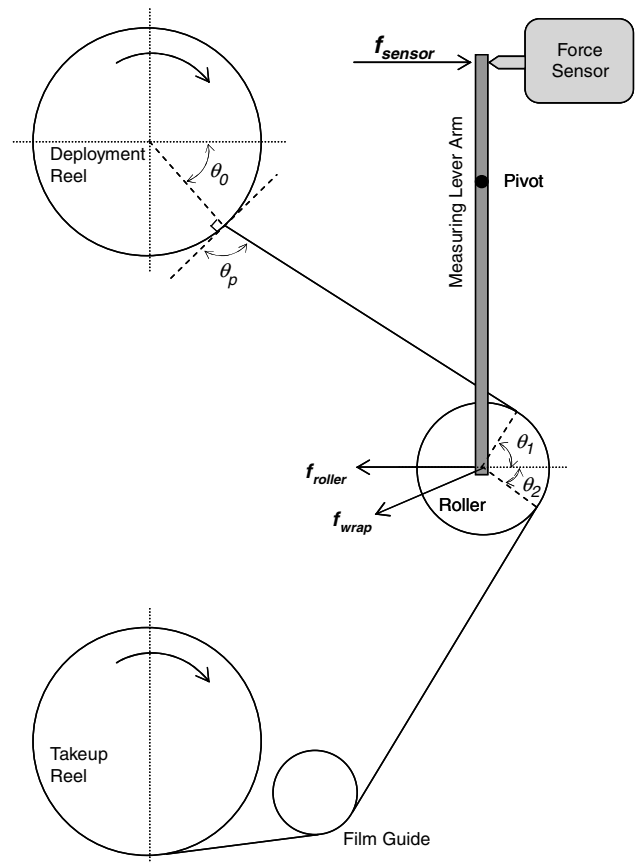

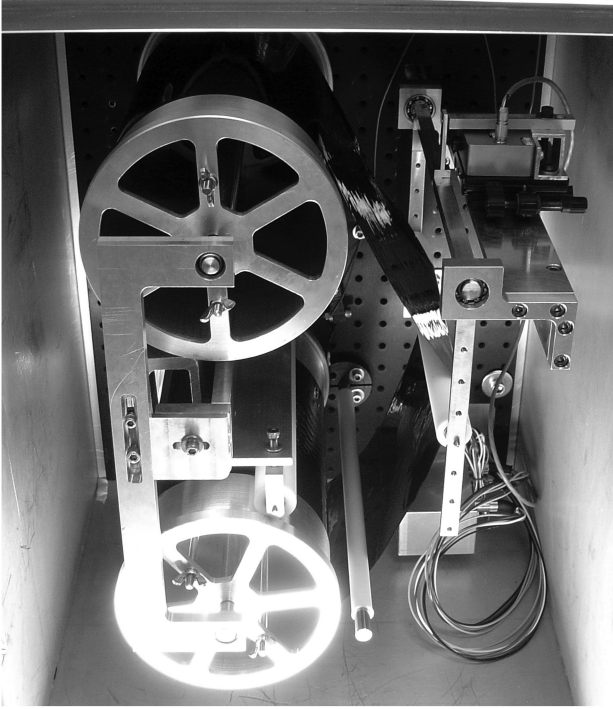**Fig. 3   Geometry of vacuum deployment experiment.**

$$f_{\text{sensor}} = R \cdot (f_{\text{roller}} + f_{\text{gravity}_{\text{film}}\text{mass}} + f_{\text{gravity}_{\text{lever}}\text{arm}} + f_{\text{friction}})$$
$$\approx R \cdot f_{\text{roller}} \tag{8}$$

In Eq. (8), the gravitational force from the mass of film sample between the reels ($f_{\text{gravity}_{\text{film}}\text{mass}}$), the lever arm restoring force from pendulum motion ($f_{\text{gravity}_{\text{lever}}\text{arm}}$), and the bearing friction force (f_{friction}) are less than the measurement accuracy, since the experiment is designed to minimize those forces. The largest $f_{\text{gravity}_{\text{film}}\text{mass}}$ is less than $2.75e - 4$ mN/m (for sample 4). The f_{friction} is less than 0.01 mN by choosing the low friction bearing. The $f_{\text{gravity}_{\text{lever}}\text{arm}}$ is almost zero, since the lever arm is designed not to move meaningfully away from its vertical position during measurements.

Because the film does not wrap symmetrically on the sensing roller about the local horizontal line, f_{wrap} and f_{roller} are different. The true force on the roller f_{wrap} can be found from f_{roller} if the two different wrap angles (θ_1 and θ_2 in Fig. 3) are known. The f_{wrap} is also described as a function of the tension T, as in Eq. (9):

$$f_{\text{wrap}} = \frac{f_{\text{roller}}}{\cos(\theta_1 - \theta_2)} = 2T \sin\left(\frac{\theta_1 + \theta_2}{2}\right) \tag{9}$$

The tension in the film can be interpreted as the force necessary to peel a film of width b off of the reel at peeling angle θ_p. Therefore, the peel force per unit width of film f_{peel} can be found using the tension, the width of the film, and the peeling angle θ_p, as shown in Eq. (10) [8]:

$$f_{\text{peel}} = \frac{T}{b}(1 - \cos \theta_p) \tag{10}$$

Note that the tension T in Eq. (10) is equivalent to F_{unroll} in Eq. (7). In the experiment, angles θ_1, θ_2, and θ_p are determined by the angle θ_0 by assuming that all of tension in the film is a result of the peel force. During the experiment, the angle θ_0 and the f_{sensor} are discretely recorded while the film is unrolled to compute the peel force and, finally, the required unrolling force.

IV. Results and Analysis

A. Thin-Film Sample Properties

NeXolve Corporation (NeXolve) is developing film variants based on Langley Research Center (LARC) CP-1 polyimide films [1]. Their casting process allows for additions in the bulk of the materials, such as Kevlar fiber. Furthermore, fillers can be added that modify the material properties of the film, thus customizing it to a particular mission. For example, carbon black can be added to the polyimide film to make it slightly conductive, thus preventing charge buildup on the film. In this research, four different samples of NeXolve CP-1 polyimide film were tested. The characteristic properties of the four samples are listed in Table 2. Samples 1 and 2 have different thicknesses of uncoated CP-1. The wrapping is very uniform, with small wrinkles developing toward both edges of the film. Because these samples are nonconductive and uncoated, significant charge buildup is expected. Therefore, two other materials (one with metal coating and the other with conductivity) were also tested.

Sample 3 has a 0.7–0.1 μm aluminum coating, which gives it a mirrorlike finish. The coating is on the top side of the film. This is the film that is most similar to what would be used on an actual solar sail mission; a perfectly reflective surface makes the most efficient solar

Fig. 4 Experimental apparatus in vacuum chamber with conductive film loaded.

peel force is extracted from an induced tension in the film during unrolling [7]. This induced tension comes about as the reels synchronously rotate, and the initial position of the peeling line rotates with the deployment reel. A dc motor and a timing belt that connects the reels make the reels rotate synchronously. Also, the reels are manufactured to have identical diameters and aligned to prevent uneven peeling along the width of the film sample. As the peeling line continues to rotate, the initial slack in the film is reduced until new film finally starts to peel off from the deployment reel and a steady state is achieved. The peel force measurement apparatus is designed to ensure the tension remaining in the moving film mostly comes from the peel force. There exist some insignificant forces that are minimized by design. The force from the mass of film between the reels is less than the sensor measurement resolution due to the low density and micrometer thickness. The force from the bearing friction is also less than the sensor measurement resolution. During the measurement, the lever arm moves slightly away from the vertical position and this pendulum motion generates pendulum restoring force. The pendulum restoring force is also minimal since very small pendulum motion is allowed in the apparatus design. As shown in Figs. 3 and 4, the film passes over a roller attached to a lever arm. This lever arm, in turn, actuates a force sensor. Because the levels of peel force were as yet unknown (but expected to be small), the lever arm ratio is designed to be adjustable. In this manner, the leverage ratio could be modified such that the small force at the roller would be magnified at the force sensor. The entire force sensor, lever arm, and roller assembly can be repositioned up or down on the rear optical mounting plate such that the roller always stays in the same position relative to the deployment and takeup reels.

C. Peel Force Derivation from Experimental Geometry

Figure 3 shows the geometry of the measurement apparatus with all of the relevant forces and angles necessary for the peel force determination labeled. The force exerted on the roller (f_{roller}) is a multiplicative factor of the measured force at the sensor (f_{sensor}), from the fact that the roller is on a lever arm to magnify the peel force. Then, if the roller is on the long arm of an R:1 lever, the force is found by Eq. (8):

Table 2 Polyimide film sample properties

Sample	1	2	3	4
Thickness, μm	3	5	3	6–7
Length, m	20	40	9.5	22
Width, mm	304.8	304.8	304.8	210
Areal density, g/m^3	4.3	7.2	7	10
Coating	——	——	0.1 μm Al	——
Surface resistivity, Ω/sq	∞	∞	1	4.5×10^5
Number of weldings	0	0	0	2

sail. Sample 4 was a 6–7-μm-thick conductive film. It is made conductive by the addition of 15% weight carbon black, rendering it totally opaque and conductive with better emissivity [2]. Sample 4 is also the only sample that is welded. Welding refers to a process that allows two separate sections of film to be joined together without the use of separate adhesives. It is nearly seamless and does not require significant overlap. Because of the low levels (nearly negligible) of peel force measured for sample 4, and the slightly less-tight contact between film layers around these welded parts, these seams should not have a significant effect on peel force measurement.

B. Peel Force Measurement

Samples 1 and 2 are tested to measure the peel force while the air pressure varies from 1 atm to 0.7 mtorr. The designed deployment speed of UltraSail is approximately 14 cm/s, and this speed allows a 500 m blade to unroll in 1 h. The deployment speed profile for sample 1 has constant acceleration/deceleration with the maximum speed of 15 cm/s. Because of the limited supply of sample 1, the deceleration starts right after the speed reaches 15 cm/s. For the tests of sample 2, three constant speeds of 0.5, 1, and 3 cm/s are used instead of varying speed. The reason for using slow speeds is to observe the static charge buildup over time.

Since samples 1 and 2 are expected to have significant charge buildup by peeling their layer, two grounded static discharge brushes are added to the top roller to combat the static buildup during the unrolling. In tests with samples 1 and 2, different static buildup phenomena are observed that depend on the air pressure. Figure 5 shows the peel force of sample 2 in a vacuum with 0.5 cm/s deployment speed. Figure 6 represents the same experiment but in atmospheric pressure. It can be seen that the peel force in atmosphere is significantly smaller than the peel force in vacuum. This difference in peel force is mostly caused by a larger static electricity buildup in
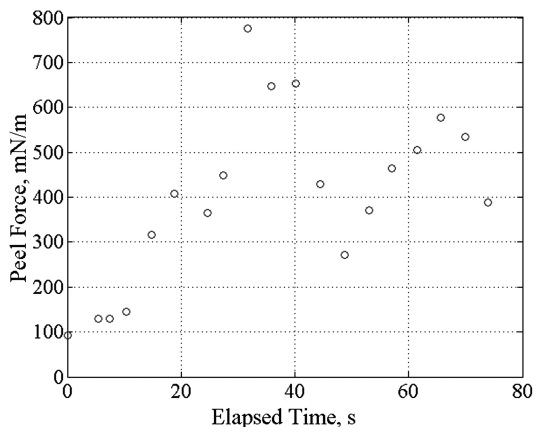
vacuum than in the air. In vacuum, the discharge brush is not able to handle the static electricity properly because of the unpredictable motion of the film. Sample 2 shows similar results with sample 1. Based on the experiment with samples 1 and 2, it is not recommended to use a nonconductive and uncoated polyimide film as a sail blade.

For the tests of sample 3 (the 0.1 μm aluminum-coated film), four different constant deployment speeds are used: 0.5, 1, 3, and 5 cm/s. Since there was no meaningful peel force or static buildup observed in sample 3 and sample 4 tests with those slow deployment speeds, and due to the limited supply of film sample, it was decided to stop increasing the deployment speed faster than 5 cm/s. The air pressure varies from 1.7 to 3.1 mtorr. The discharging brushes are not used. As shown in Fig. 7 through the sensor voltage output, there is a negligibly small peel force. During sample 3 tests, the initial slack that is left in the film is never taken up, so there is no tension on the film. That means that the peel force is less than the force of gravity acting on the thin film in the peeling region. There is also no perceptible charge buildup or static phenomena observed. Figure 7 shows the measured force sensor voltages. Voltage measurements from multiple tests are within the error of the data acquisition device. This means that the level of force, if there is any, is well below the threshold measurable by the experiment system (1 mN/m). The reason that voltage differences are displayed in Fig. 7 instead of the actual peel force is because the peel force cannot be calculated if there is no tension in the film.

The test results of sample 4 (the conductive film) are similar with the tests with sample 3. Various constant deployment speeds up to 5 cm/s are used with the air pressure varying from 1.1 to 2.9 mtorr. Similarly, with Fig. 7, the voltage measurements are centered around zero and are within the accuracy limits of the data acquisition device. This means that the peel force for this conductive film sample is less than the threshold measurable by the experiment system.

In the vacuum deployment experiments, it is shown that for a typical solar sail film sample (i.e., a coated or coated/conductive polyimide film), the peel force is near zero. The zero peel force makes further design of the deployment mechanism easier. In the baseline deployment design, the tension on the blade must be kept at all times to have a controlled deployment. With the zero peel force, a small amount of tension could be put in the film by means of a brake or a motor attached to the deployment reel. Then, because the peel force is near zero, the film would peel off the reel as controlled by the motor. The deployment speed is easily controlled in this manner.

C. Pressure Variation by Trapped Air

It is observed that the chamber pressure rises slightly during the experiments. This rise in chamber pressure is closely correlated to the actual time that the unrolling of the film occurred, i.e., when the rollers are in motion. A typical pressure increase for one such experiment is shown in Fig. 8. The delayed rise in pressure (pressure

Fig. 5   Peel force of sample 2 (uncoated): 0.5 cm/s, 0.9 mtorr.

Fig. 6   Peel force of sample 2 (uncoated): 0.5 cm/s, 1 atm.
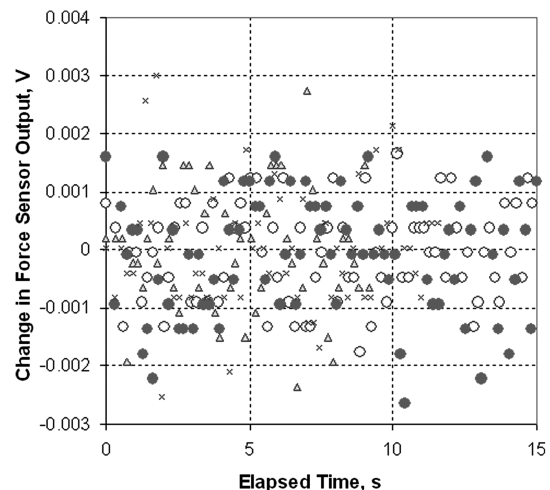

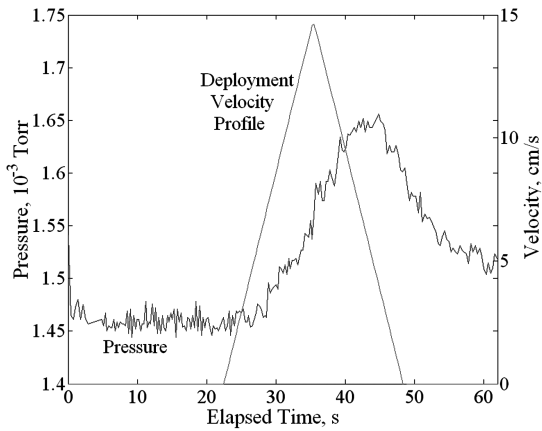Fig. 7   Peel force of sample 3 (coated with aluminum): 1.7 to 3.1 mtorr.

Fig. 8   Pressure increase during the unrolling using sample 1.
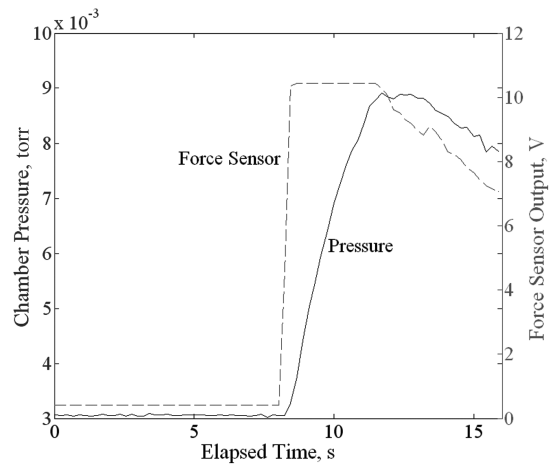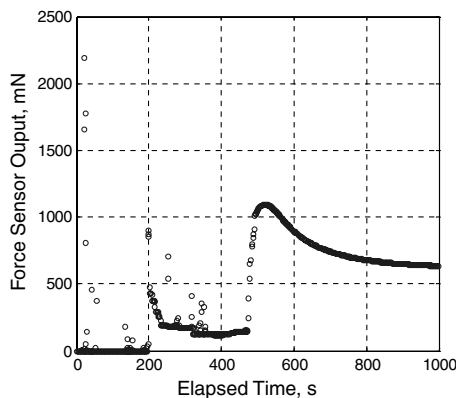

Fig. 9   Pressure and measured force jumps during a sudden gas release of sample 3.

rise is slightly offset from velocity profile) is due to the response time of the vacuum gauge and the diffusion time of the newly introduced gas into the chamber.
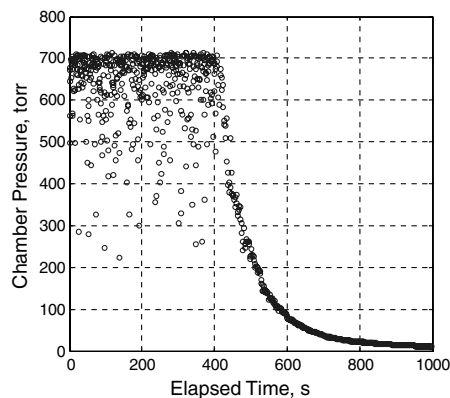
For an experiment performed on sample 3 (the aluminum-coated film), a release of trapped air between film layers is observed. During the first part of the experiment, the peel force appeared to be the same, negligible amount as in other sample 3 experiments. This initial peel force can be seen during 0 to 8 s in Fig. 9. Then, almost instantaneously, the measured force sensor voltage spikes to the force sensor's saturation level. This increase in the measured force happened in less than half a second. A significant jump in chamber pressure is observed at the time during the experiment. This pressure history can be also seen in Fig. 9 and correlates with the rise in force.

The slight (4 s) delay between the force spike and the pressure rise is again due to the response time of the vacuum gauge and the way in which the gas escaped from the bubble.
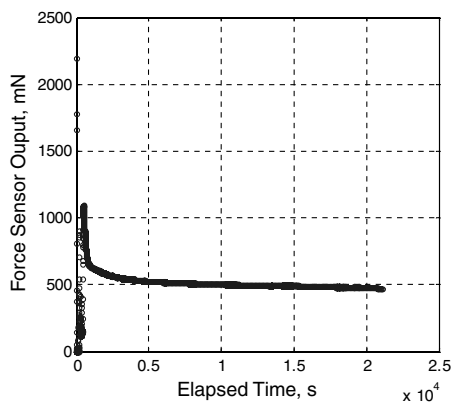
The trapping of air between the layers can occur during fabrication and the winding process, or the air made its way between the layers while the film roll is stored and is later trapped as the chamber is evacuated. The former theory would tend to explain a larger-sized gas pocket, while the latter might better explain a slow steady source of gas as the film is deployed under vacuum. In any case, it is possible for pockets of air at atmospheric pressure to remain in the wrapped film even after the chamber is pumped down.
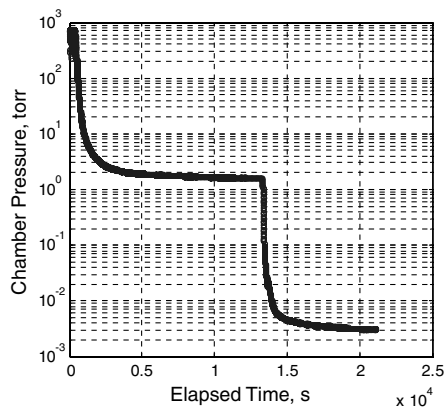

a) Force sensor for t < 1000 s

b) Pressure for t < 1000 s

c) Force sensor for 0 < t < 20,000 s

d) Force sensor for 0 < t < 20,000 s

Fig. 10   Force sensor voltage and pressure history during the first pumpdown for sample 4 test.

D. Film Shrinkage by Outgassing in Sample 4

During the first pumpdown for the test of sample 4, the output for the force sensor voltage and the air pressure vary as shown in Fig. 10. Figures 10a and 10b show the close-up of initial 1000 s of force sensor voltage and pressure history, while Figs. 10c and 10d show the next 20,000 s (5.55 h) of pumpdown time. During the pumpdown, the motor is engaged and energized to hold the reels at the initial position. Therefore, the observed force does not come from the peel force or static electricity but potentially from film shrinkage by an outgassing process as well as the expansion of trapped air. The outgassing and escape of loosely trapped air are observed in Fig. 10b. For the first 20 min, the chamber pressure is approximately atmospheric, but it should have been rapidly decreasing if there is no air supply into the chamber. The large drop in pressure seen in Fig. 10d indicates that an equilibrium is finally reached; the exposed film could not outgas any more. Thus, the pumps could effectively evacuate the chamber. The outgassing is not observed in subsequent experiments on sample 4 after the initial pumpdown.

It is postulated by the manufacturer of the film, NeXolve, that the shrinkage may be caused by the curing process [4]. The carbon loaded films may have absorbed more water than the other films during the curing. Upon release of this water, the film shrunk. This type of shrinkage may have significant implications on the UltraSail system. It is estimated that the amount of shrinkage is on the order of a few percent in length, so a corresponding amount of extra film needs to be available to compensate for the shrinkage. In effect, this might reduce the achievable accelerations for a given set of UltraSail design parameters, and the launch mass will be increased unnecessarily.

Experiments with sample 3 and sample 4 identified potentially serious complications that could arise during sail deployment. The sudden gas escape is certainly not desirable in a space environment. In the experiment, it affects every layer of film on the reel by moving it and wrinkling the inside layers. Furthermore, the escape itself is quite violent. The potential problems caused by the film shrinkage are already discussed. One of the solutions to these problems is to add microperforations or holes in regular positions along the width of the film. More studies need to be performed to determine the optimal position, size, frequency, and pattern of the perforations for balanced ventilation capacity and tensile strength. Also, more studies are required to find the composition and amount of gas from the outgassing for further design of the UltraSail.

V.   Conclusions

A thin-film deployment experiment and custom vacuum chamber were developed for this research. The deployment apparatus can safely simulate deployment speed up to 15 cm/s, but it has the capability to deploy at 100 cm/s. Four thin-film samples have been tested for peel force in a vacuum environment. The irregular electrostatic forces on uncoated, nonconductive films (samples 1 and 2) caused large and unpredictable peel forces. This result implies that uncoated/nonconductive film is not suitable for this application, from the standpoint of its ability to unroll. However, besides its demonstrated large peel force, the uncoated/nonconductive film is not suitable for a real solar sail mission because it cannot provide the requisite reflectivity. The electrically conductive samples 3 and 4 displayed no measurable peel force. This result is critical in designing the deployment mechanism. Also, it was shown that the trapped air between the layers of film should be avoided. Further study is required on how to minimize the size of trapped air. There exists a threshold on the minimum measurable peel force in a gravitational field (e.g. on the ground). Therefore, if desired, a reduced-gravity experiment could enable the measurement of this very small peel force.

References

[1] Talley, C., Clayton, W., Gierow, P., McGee, J., and Moore, J., "Advanced Membrane Materials for Improved Solar Sail Capabilities," AIAA Paper 2002-1561, 2002.

[2] Connell, J. W., Smith, J. G., Jr., Watson, K. A., and Delozier, D. M., "Space Durable Polyimide/Carbon Nanotube Composite Films for Potential Applications on Gossamer Spacecraft," AIAA Paper 2004-1779, 2004.

[3] Burton, R. L., and Coverstone, V. L., Hargens-Rysanek, J., Ertmer, K. M., Botter, T., Carroll, D. L., Benavides, G., and Woo, B., "UltraSail: Ultra-Lightweight Solar Sail Concept," AIAA Paper 2005-4117, 2005.

[4] Ertmer, K. M., "Design and Operation of A Thin-Film Vacuum Deployment Experiment for UltraSail Concept Validation," M.S. Thesis, Department of Aerospace Engineering, Univ. of Illinois at Urbana–Champaign, Urbana, IL, 2006.

[5] Hargens-Rysanek, J., Coverstone, V. L., and Burton, R. L., "Orbital Precession Via Cyclic Pitch for the UltraSail System," American Astronomical Soc. Paper 07-166, Washington, D.C., 2007.

[6] Kendall, K., *Molecular Adhesion and Its Applications: The Sticky Universe*, Plenum Press, New York, 2001, pp. 25–34.

[7] Hawkins, W. E., *The Plastic Film and Foil Web Handling Guide*, CRC Press, London, 2003, Chaps. 2, 3.

[8] Kendall, K., "Thin-Film Peeling: The Elastic Term," *Journal of Physics D: Applied Physics*, Vol. 8, 1975, pp. 1449–1452. doi:10.1088/0022-3727/8/13/005

P. Gage
Associate Editor